Proceedings of the 2010 IEEE
International Conference on Mechatronics and Automation
August 4-7, 2010, Xi'an, China

Modeling and Control of a Bi-brachiate Inspection Robot for Power Transmission Lines

Guodong Yang, En Li, Changchun Fan, Weiyang Lei and Zize Liang

Abstract— **This paper presents the framework, modeling, controller design, simulation and experiment results of a bi-brachiate inspection robot, which is designed to inspect the high voltage power transmission lines. A bionic structure is adopted for the mechanical design of the inspection robot. It has two multi-joint arms with a claw and a wheel on the top of each arm. A counterweight box is designed to adjust its center of mass (COM). With the wheels it can ride along the line when there are no obstacles. Once it encounters obstacles, the robot can negotiate the obstacle with a turning around way. In order to design a feedback control law, the simplified model of the robot body and its dynamic equation have been developed. Based on the models, an adaptive control law using fuzzy compensator is described in detail. Simulation and experiment results show the effectiveness of the control law and the designed robot prototype.**

I. INTRODUCTION

Maintenance and periodic inspection of the power transmission lines are becoming more and more significant to insurance the reliable electric power supply. Currently, these tasks are carried out mainly by two ways, workers and helicopters [1]. However, the manual way is a waste of time and is also dangerous for workers because of the wide and various terrain, while the other way is costly and requires many strict conditions, such as the weather, the skill level of the pilot and so on. Nowadays, with the development of robotics, inspection by robot has drawn a lot of attentions from researchers all around the world.

Research on the inspection of the power transmission lines using automatic devices has emerged since the late 1980s. Sawada et al.[2] designed an inspection robot that can navigate the ground line located above the actual power transmission lines. It is equipped an arc-shaped arm as a guide rail by which the robot can negotiate the obstacles on the lines. When the robot encounters obstacles such as tower, it unfolds the arc-shaped arm and attaches its body to the other side of the tower, then the robot can travel along the arm to cross the tower. Montambault and Pouliot [3] developed an inspection robot capable of clearing obstacles while operating on live lines. It can move along several axes, and adjust its shape in real time according to various line configurations and obstacles. The robot can run on the energized line for a long time and can be remotely operated from 5 km away. It has the ability of learning to clear obstacles by means of automated sequences. Wu et al. [4] designed an inspection robot with double-arms-symmetric suspension structure. It has two electro-magnetic sensors installed on each arm which can detect, identify, and localize obstacles. A motion planning strategy is applied to compute the non-collision path and the corresponding joint angles.

Since 2002, a great deal of work about inspection robot has been done in our laboratory including robot framework design, obstacle negotiation, obstacle recognition, etc. Liang et al. [5] designed a tribrachiation mobile robot and a hierarchical control system with an embedded controller by which the robot can negotiate obstacles automatically. A recursive CCD method is used to solve the constrained inverse kinematics problem of the robot, and motion planning is done using hierarchical planning method by combining behavior reasoning and motion interpreting. Fu et al. [6] proposed a visual obstacle recognition algorithm based on the structure of the 220 KV power transmission line. The algorithm is composed by a straight line extraction algorithm and a circle or ellipse extraction algorithm utilizing the notion that the structure of all the obstacles in the line are circular or elliptic and that of the background objects are straight line. Li et al. [7] described a brachiation mobile robot. By analyzing the ball and beam model of the robot, a set-point balance control approach is presented. The control law is designed based on the total mechanical energy and the passivity properties of the system. According to the desired set-point, the zero equilibrium point and the nonzero equilibrium points are studied respectively.

In this paper, a bi-brachiate inspection robot which can autonomously negotiate the obstacles in a turning around way is introduced. The robot framework is described in detail as well as its obstacle negotiation procedures. The dynamics of the robot when crossing the obstacles is studied and its dynamic equation is given based on the simplified model. Because the major uncertainty of the robot is the friction generated by rotation of the joint, a fuzzy system is presented to approximate and compensate the friction, and the adaptive control law of the robot is derived based on the approximation and implemented on a real time embedded system. Finally, the simulation and experimental results are depicted in detail.

II. SYSTEM DESCRIPTION

The bi-brachiate inspection robot prototype is shown in Fig. 1. It adopts a bionic structure with two arms and a counterweight box. Each arm has a wheel driven by running motor which makes the robot capable of riding along the power lines and three rotating joints which are the clamping

This work is supported by the National High Technology Research and Development Program of China, Grant #2007AA041501 and #2007AA041502.

G.Yang,E.Li,C.Fan,W.Lei&Z.Liang are with the Key Laboratory of Complex Systems and Intelligent Science, Institute of Automation, Chinese Academic of Sciences, Beijing 100190, China guodong.yang@ia.ac.cn

978-1-4244-5141-8/10/$26.00 © 2010 IEEE

joint, the swaying joint and the turning joint. The clamping joint has a claw which can grasp the power lines utilizing a leverage. The swaying joint can adjust the robot's attitude by swaying it up and down to grasp the line exactly. The turning joint can turn the robot body around one arm to negotiate obstacles. Keeping the COM of the robot along the rotating arm is very important, or damages will be caused to the robot framework because the whole weight of the robot is pressed on the clamping joint when it takes the obstacle negotiation procedure. That is the reason to design the counterweight box. By moving the counterweight box along the guide rail, the COM of the robot will be always kept on the same line of the rotating arm and downwards it, guaranteeing the robot on its right posture. Fig. 2 shows the detail structure of the inspection robot.

To fulfill the maintenance and inspection task, the robot must be able to get across the obstacles installed on the power lines, such as the vibration dampers, the insulator strings, the suspension clamps, and so on. When the robot encounters obstacles, it takes procedures as follows:

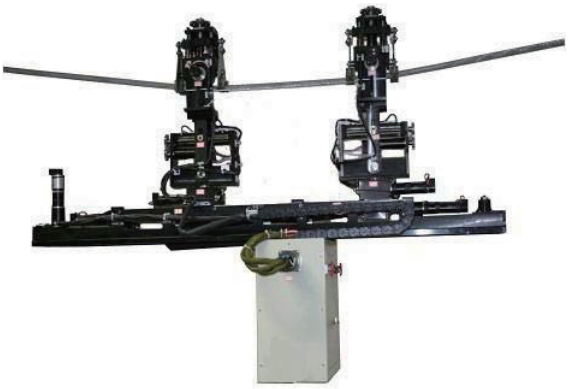

Fig. 1: Prototype of the inspection robot

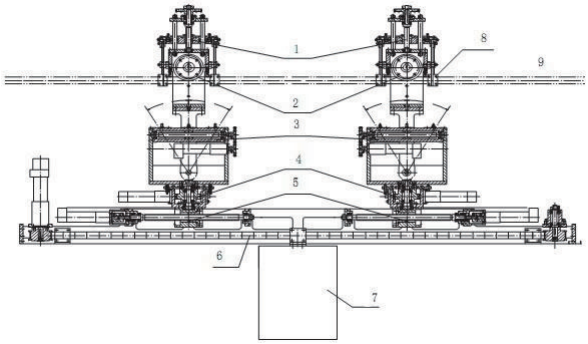

Fig. 2: Structure of the inspection robot: 1, the clamping joint. 2, the wheel. 3, the swaying joint. 4, the turning joint. 5, distance adjusting joint. 6, guide rail. 7, counterweight box. 8, claw. 9, power transmission line

1) Close the claw of the forearm (closed to the obstacle) to grab the power line. Move the counter-weight box to the front end (closed to the obstacles) of the guide rail. To simplify the operation, here the counterweight box is just moved to the front end of the guide rail instead of continuous moving to adjust the COM of the robot. 2) Sway up the robot body by the swaying joint of the forearm, so the claw of the rear arm can get off the power line. 3) Turn the robot body around the forearm to get across the obstacle by the turning joint of the forearm. 4) Sway down the robot to make the wheel of the rear arm hanging on the power line by the swing joint of the forearm. 5) Close the claw of the rear arm to grab the power line. Now the robot has one arm across the obstacle and the other behind it. 6) Repeat procedure 1)∼5) to the rear arm, then the whole robot body can get across the obstacle.

The ultimate goal of the robot is to accomplish the maintenance and inspection works automatically, that is to say the robot has the ability to negotiate obstacles and ride on the power lines freely. A closed-loop controller is designed based on the adaptive fuzzy logic, which can synthesis the inputs of desired trajectory and sensor signals and give the right output to the DC motors by pulse-width-modulated (PWM) waveforms. The diagram of the controller is shown in Fig. 3. Cameras are mounted on the robot framework

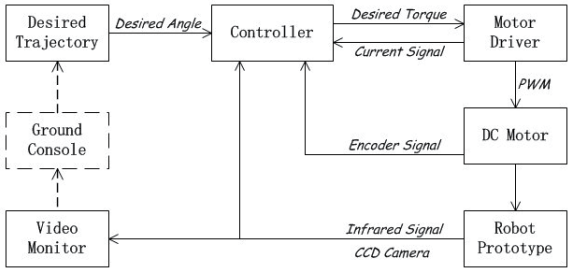

Fig. 3: Diagram of the robot controller

and the video signals are transported to the ground console as a supervision of the inspection procedures, especially the obstacle negotiation. The controller is executed on a embedded real-time system, as shown in Fig. 4. The hardware system contains an ARM chip as the central processor, and a FPGA chip as the coprocessor. Control algorithm is executed on ARM, and all the sensor signals are processed on FPGA. The system can drive 12 DC motors by closed loop to perform a complete control of the inspection robot.

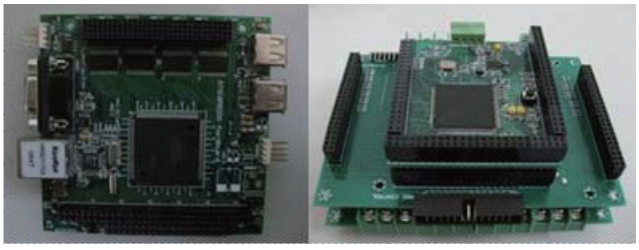

Fig. 4: Hardware system of the robot controller

III. MODELING

The most difficult part of the inspection by robot is automatic obstacle negotiation. So we only consider the modeling during the obstacle negotiation procedure. As described in last section, the robot takes a turning-around way while getting across the obstacles with one arm grasping the power line and the other turning around it. The counterweight box is fixed to the front end of the guide rail to simplify the operation. So the robot model can be simplified to a special two-link manipulation, as shown in Fig 5.

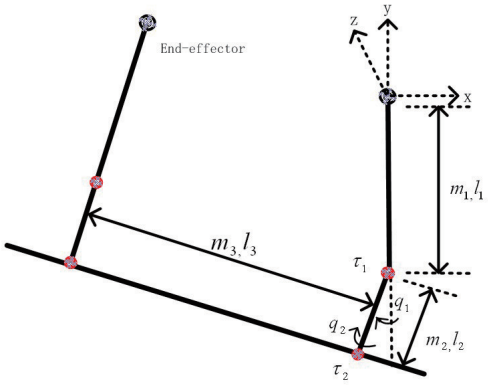

Fig. 5: Simplified model of the robot

The dynamics of the model can be derived by the Lagrange's equations, as:

$$\frac{d}{dt}\frac{\partial L}{\partial \dot{q}_i} - \frac{\partial L}{\partial q_i} = \tau_i \ , \quad i = 1, \cdots, n \tag{1}$$

where

$$L = K - P \tag{2}$$

is the Lagrangian expressed as the difference between kinetic energy K and potential energy P, τ_i is the generalized force at joint i, and q_i is the angle of ith joint, and all the joints considered in the model are revolute joints. From (1) and (2), the dynamic equation of the robot can be derived as follows:

$$M(q)\ddot{q} + C(q,\dot{q})\dot{q} + G(q) = \tau \tag{3}$$

where

$$M = \begin{bmatrix} m_{11} & m_{12} \\ m_{21} & m_{22} \end{bmatrix}, C = \begin{bmatrix} c_{11} & c_{12} \\ c_{21} & c_{22} \end{bmatrix}, G = \begin{bmatrix} g_1 \\ g_2 \end{bmatrix}$$

$$q = \begin{bmatrix} q_1 \\ q_2 \end{bmatrix}, \tau = \begin{bmatrix} \tau_1 \\ \tau_2 \end{bmatrix}$$

$$\begin{aligned} m_{11} &= (m_1 + m_2 + \frac{1}{3}m_3)l_3^2 \cos^2 q_2 + (\frac{1}{3}m_1 + \frac{2}{3}m_2 + m_3)l_2^2 \\ &\quad + \frac{1}{3}(m_1 + m_2)(l_1^2 - l_1 l_2) \\ m_{12} &= \frac{1}{2}((m_1 + m_2)l_1 - (m_1 + m_2 + m_3)l_2)l_3 \sin q_2 \\ m_{21} &= m_{12} \\ m_{22} &= \frac{1}{3}l_3^2 \sin^2 q_2 + (m_1 + m_2)l_3^2 \\ c_{11} &= -2(m_1 + m_2 + \frac{1}{3}m_3)l_3^2 \dot{q}_2 \cos q_2 \sin q_2 \\ c_{12} &= \frac{1}{2}((m_1 + m_2)l_1 - (m_1 + m_2 + m_3))l_3 \dot{q}_2 \cos q_2 \\ c_{21} &= (\frac{1}{4}(m_1 + m_2)l_1 \dot{q}_2 - \frac{1}{4}(m_1 + m_2 + m_3)l_2 \dot{q}_2 \\ &\quad + (m_1 + m_2 + \frac{1}{3}m_3)l_3 \dot{q}_1 \sin q_2)l_3 \cos q_2 \\ c_{22} &= (-\frac{1}{4}(m_1 + m_2)l_1 \dot{q}_1 + \frac{1}{3}m_3 l_3 \dot{q}_2 \sin q_2 \\ &\quad + \frac{1}{4}(m_1 + m_2 + m_3)l_2 \dot{q}_1)l_3 \cos q_2 \\ g_1 &= (\frac{1}{2}(m_1 + m_2)l_1 + (\frac{3}{2}m_1 + \frac{5}{2}m_2 + m_3)l_2)g \sin q_1 \\ &\quad + (m_1 + m_2 + \frac{1}{2}m_3)g l_3 \cos q_1 \cos q_2 \\ g_2 &= -(m_1 + m_2 + \frac{1}{2}m_3)g l_3 \sin q_1 \sin q_2 \end{aligned}$$

Where $M(q)$ is the symmetric positive-definite inertia matrix, $C(q,\dot{q})$ is the centripetal and Coriolis torques and $G(q)$ represents the gravitational torques. m_1 denotes the mass between the claw and the swaying joint of one arm, m_2 denotes the mass between the swaying joint and the turning joint of the arm, m_3 denotes the mass of the guide rail of the robot, and l_1, l_2, l_3 are their length respectively. g is the acceleration of the gravity. q_1 denotes the swing angle between the vertical direction and the link between the swaying joint and the turning joint. q_2 denotes the rotary angle of the relative turning joint. τ_1 and τ_2 are the input forces of the swaying joint and the turning joint. Consider the effectiveness of uncertainty, such as friction, disturbance and so on, (3) can be rewritten as:

$$M(q)\ddot{q} + C(q,\dot{q})\dot{q} + G(q) + F_r(q,\dot{q},\ddot{q}) = \tau \tag{4}$$

Where $F_r(q,\dot{q},\ddot{q})$ is the uncertain term depending on the joint angle, velocity and acceleration. As we can see that all the system parameters are fixed except F_r. So before designing the system control law, the uncertain term must be compensated. In the following section, a fuzzy system is designed to approximate the uncertainty of the robot.

IV. CONTROL DESIGN

The simplified dynamic model of the robot (4) can be regarded as a multi-input multi-output(MIMO) nonlinear system, which has the properties of nonlinear, unstable and uncertainty. Based on practical operation, the major uncertainty is caused by friction of the rotation of each joint, and the dynamics of the friction is hardly described precisely. In this paper, a friction compensator based on fuzzy logic is designed to approximate the actual friction dynamics, and system control law is derived based on the method described in [10]. The properties of the adaptive fuzzy logic about approximating continuous functions over a compact set to an arbitrary degree of accuracy if enough number of rules have been considered [9] and making use of

linguistic information in a systematic way [8] insurance the feasibility of the presented method.

A. Fuzzy System

Let the fuzzy system be a mapping from $U \subseteq R^n$ to R, where $U = U_1 \times \cdots \times U_n,\ U_i \subset R,\ i = 1,\ 2, \cdots,\ n$. The input vector is $x = [x_1, \cdots,\ x_n]^T \in U \subset R^n$ and the output variable is $y \subset R$. Then the lth rule of the fuzzy system can be described as a set of if-then rules in the following form:

$$R^l:\ \text{if } x_1 \text{ is } F_1^l \text{ and } \cdots \text{ and } x_n \text{ is } F_n^l,\ \text{then } y^l \text{ is } C^l \tag{5}$$

where $F_i^l,\ l = 1, \cdots,\ M$ denotes the fuzzy set defined on the universe of discourse of the ith input, and C^l is a fuzzy set defined on R.

By utilizing the singleton fuzzifier, product inference engine, and center-average defuzzifier, the output of the fuzzy system can be shown as:

$$y(x) = \frac{\sum_{l=1}^{M} \bar{y}^l \left(\prod_{i=1}^{n} \mu_{F_i^l}(x_i) \right)}{\sum_{l=1}^{M} \left(\prod_{i=1}^{n} \mu_{F_i^l}(x_i) \right)} \tag{6}$$

where $\bar{y}_l$ is the point at which the membership function μ_c^l achieves its maximum value, and $\mu_c^l(\bar{y}^l) = 1$.
Equation(6) can be rewritten as follows:

$$y(x) = \xi^T(x)\theta \tag{7}$$

where $\theta = [y^1, \cdots, y^M]^T$ is a vector of the adaptive parameters, and $\xi(x) = [\xi_1(x), \cdots, \xi_M(x)]$ is a set of fuzzy basis functions defined as:

$$\xi_l(x) = \frac{\prod_{i=1}^{n} \mu_{F_i^l}(x_i)}{\sum_{l=1}^{M} \left(\prod_{i=1}^{n} \mu_{F_i^l}(x_i) \right)} \tag{8}$$

With the property of universal approximation of the fuzzy system described above, the uncertainty due to friction, disturbance, etc. is approximated and compensated by an adaptive compensator based on fuzzy logic.

B. Control Design

As we know, the major uncertainty is caused by friction of the joint rotation, and the friction is a local effect generated only by the joint's own angular velocity, which means joints of the robot model are independent and uncoupled in friction. So (4) can be rewritten as:

$$M(q)\ddot{q} + C(q,\dot{q})\dot{q} + G(q) + \hat{F}_r(\dot{q}) = \tau \tag{9}$$

Where $\hat{F}_r(\dot{q})$ is the designed fuzzy system to approximate the real friction model. Define the sliding surface function as:

$$s(t) = \dot{e}(t) + \Lambda e(t) \tag{10}$$

Where Λ is positive-definite matrix, $e(t) = q(t) - q_d(t)$ denotes the trajectory error. From (10), one can get the conclusion that $e(t) \to 0$ asymptotically if $s(t) \to 0$. In order to derive the sliding mode control law such that the sliding mode exists on $s = 0$, a vector of self-defined reference variables is presented as:

$$\dot{q}_r(t) = \dot{q}_d(t) - \Lambda e(t) \tag{11}$$

Then the system control law can be derived as:

$$\tau = M(q)\ddot{q}_r + C(q,\dot{q})\dot{q}_r + G(q) + \hat{F}_r(\dot{q}|\theta) - K_D s \tag{12}$$

Where $K_D = diag(K_i)$, $K_i > 0$, $i = 1, 2$. And the approximating fuzzy system is represented as:

$$\hat{F}_r(\dot{q}|\theta) = \begin{bmatrix} \hat{F}_{r1}(\dot{q}_1) \\ \hat{F}_{r2}(\dot{q}_2) \end{bmatrix} = \begin{bmatrix} \theta_1^T \xi_1(\dot{q}_1) \\ \theta_2^T \xi_2(\dot{q}_2) \end{bmatrix} \tag{13}$$

The adaptive law of θ is designed as:

$$\theta_i = -\Gamma_i^{-1} s_i \xi_i(\dot{q}_i), \qquad i = 1, 2 \tag{14}$$

Where Γ is the update rate of the presented fuzzy system. $\xi(\dot{q})$ is the vector derived by substituting $\dot{q}$ into the fuzzy basis function $\xi(x)$ mentioned above.

V. RESULT

In this section, the simulation results of the simplified model and the laboratory experiment results are presented.

A. Simulation

To examine the effectiveness of the provided controller, simulations are carried out using Matlab/Simulink. When it encounters obstacle while riding along the power line, the robot first closes the claw of the forearm and sways up the other end to get off the power line, then turns around the forearm to cross the obstacle and sways down the robot to get on the power line simultaneously. Based on the actual operation procedure, the maximum swaying angle is set to $\pi/18$ and the maximum turning angle is set to π. The desired trajectory of the robot end-effector can be formulated as:

$$q_{d1}(t) = \begin{cases} \pi t/180 & t \le 10 \\ \pi/18 - \pi(t-10)/540 & 10 < t \le 40 \\ 0 & t > 40 \end{cases}$$

$$q_{d2}(t) = \begin{cases} 0 & t \le 10 \\ \pi(t-10)/30 & 10 < t \le 40 \\ \pi & t > 40 \end{cases}$$

The system parameters are given as: $m_1 = 10kg$, $m_2 = 2.5kg$, $m_3 = 20kg$, $l_1 = 0.4m$, $l_2 = 0.1m$, $l_3 = 0.8m$, $\Lambda = diag(30,\ 30)$, $K_D = 10I_2$, $\Gamma_1 = \Gamma_2 = 0.0001$. The friction model is designed as:

$$F_r(\dot{q}) = \begin{bmatrix} 10\dot{q}_1 + 2sign(\dot{q}_1) \\ 15\dot{q}_2 + 3sign(\dot{q}_2) \end{bmatrix}$$

and the membership functions are given as:

$$\mu_{F_i^1}(x_i) = \exp\left(-\frac{1}{2} \left(\frac{x_i + 0.5}{10} \right)^2 \right)$$

$$\mu_{F_i^2}(x_i) = \exp\left(-\frac{1}{2} \left(\frac{x_i + 0.25}{10} \right)^2 \right)$$

$$\mu_{F_i^3}(x_i) = \exp\left(-\frac{1}{2} \left(\frac{x_i}{10} \right)^2 \right)$$

$$\mu_{F_i^4}(x_i) = \exp\left(-\frac{1}{2} \left(\frac{x_i - 0.25}{10} \right)^2 \right)$$

$$\mu_{F_i^5}(x_i) = \exp\left(-\frac{1}{2} \left(\frac{x_i - 0.5}{10} \right)^2 \right),\ i = 1,\ 2,\ 3,\ 4,\ 5$$

The simulation results of position tracking are shown in Fig. 6, and the position tracking error results are shown in Fig. 7. From these results we can see that the proposed controller can tracking the desired trajectory very well and the tracking error is negligible. Fig. 8 shows the approximation result of the friction model, which also indicates the good performance of the proposed fuzzy system and the uncertainty caused by joint friction can be alleviated effectively. The oscillation at the sudden change of angular velocity in Fig. 8 indicates the direction of further study. By adjusting the parameters of the fuzzy system, such as decreasing the update rate or increasing the number of fuzzy rule, we can get better approximation results as well as more system burden which will affect the performance of the real time system. How to balance the approximation result and the real time performance is the key point in the future work.

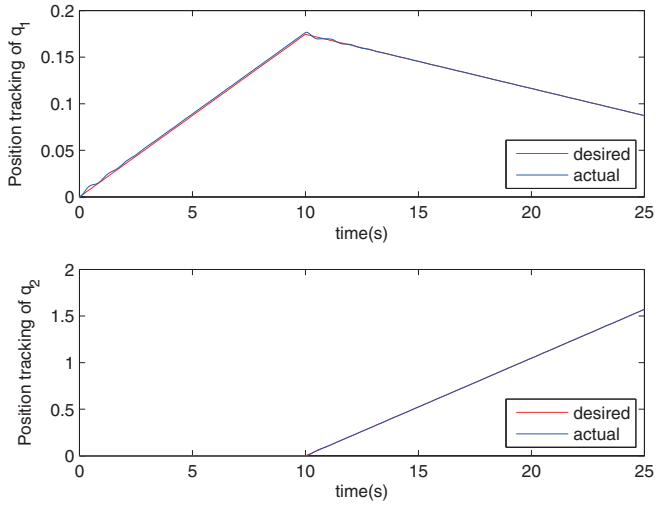

Fig. 6: Position tracking of q_1 and q_2

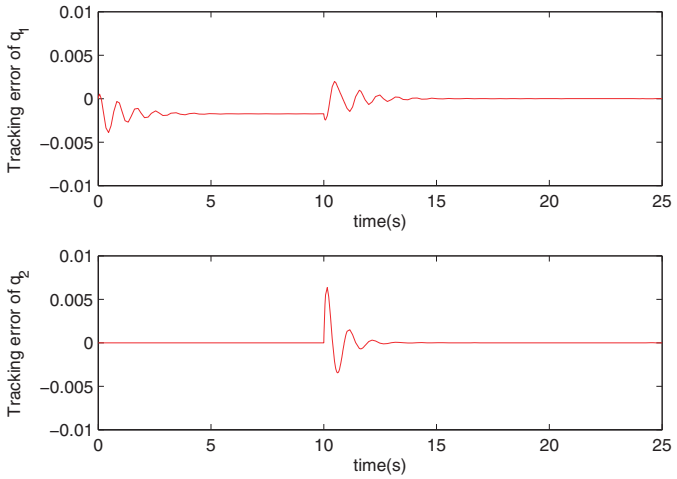

Fig. 7: Tracking error of q_1 and q_2

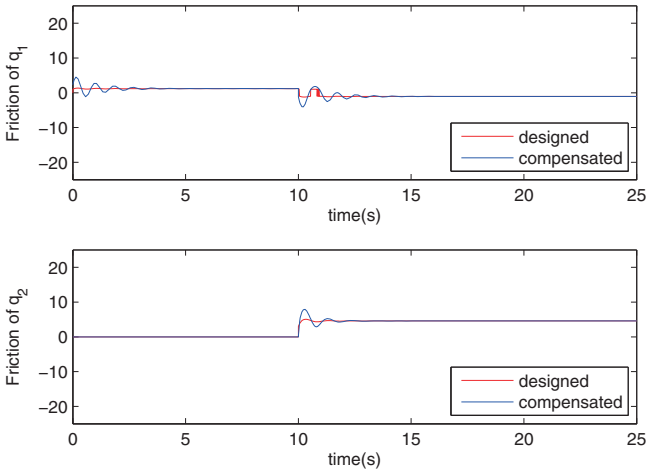

Fig. 8: Friction and its compensation of q_1 and q_2

B. Laboratory Experiment

The control algorithm has been applied to the robot prototype shown in Fig. 1 and executed on a real time embedded system composed mainly by ARM and FPGA chips, as shown in Fig. 4. ARM is the central processor handling all the relative information and the obstacle negotiation procedure. FPGA is the coprocessor dealing with the sensor signals such as the optical encoder and generating PWM waveforms to control the motors. The desired trajectory is set in ARM, and the actual trajectory is calculate by FPGA based on the information from optical encoder. Experiments have been taken in the laboratory, where power transmission apparatus are installed including the power lines and several obstacles such as vibration dampers and suspension clamps. Fig. 9 shows the procedure of the robot negotiating a suspension clamp. As we can see, when it encounters obstacle, the robot prototype can take procedures and negotiate the obstacle automatically.

VI. CONCLUSION

Power transmission line inspection using robotic technology has drawn more and more attentions, and lots of inspection robots have been developed since 1980s. In this paper, a bi-branchiate robot for the inspection of the power transmission lines and the implemented control algorithm are described. The robot adopts a turning around way with one arm hanging on the power line and the other turning the robot body around it when negotiating obstacles, which makes it capable of crossing all the obstacles installed on the power line without considering the type of obstacles. The major uncertainty of the system is the friction caused by the rotation of the joints, while the other system parameters are assumed to be known exactly. A fuzzy system is designed to approximate the friction dynamics and compensate it. An adaptive control algorithm based on the fuzzy approximation system is designed and implemented on the real time embedded system. Simulation and laboratory

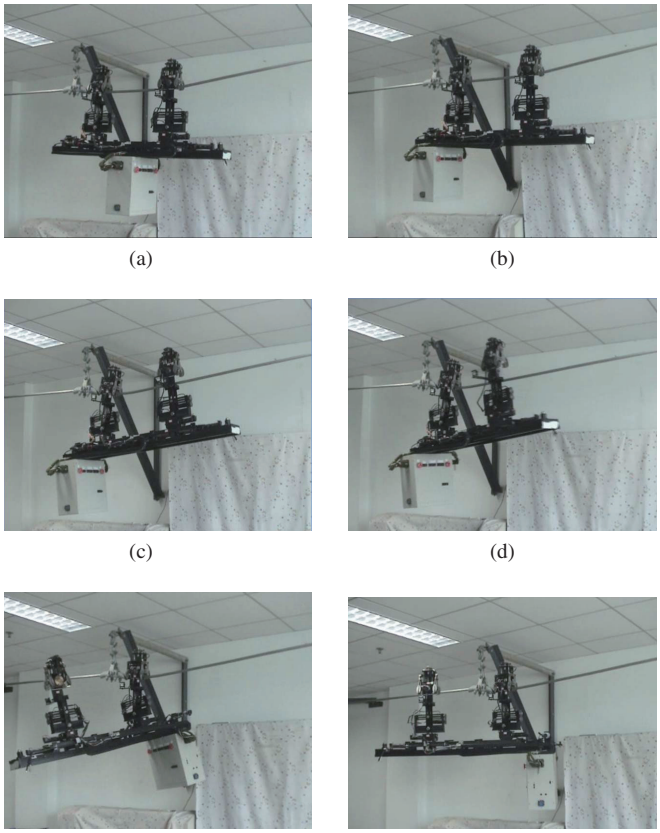

Fig. 9: Suspension clamp negotiation: (a) robot encounters obstacle. (b) close the claw of forearm and move the counterweight box. (c) sway up the rear arm. (d) turn around the forearm. (e) continue turning. (f) the rear arm has crossed the obstacle.

experiment results are presented, which show the effectiveness of the robot prototype and the control algorithm.

REFERENCES

[1] Y. Ch. Zhang, Z. Z. liang and M. Tan, "Mobile robot for overhead powerline inspection - a review," *Robot*, vol. 26, no. 5, 2004, pp. 467-473.

[2] J. Sawada, K. Kusumoto, T. Munakata, Y. Maikawa, Y. Ishikawa, "A mobile robot for inspection of power transmission lines," *IEEE Trans. Power Delivery*, vol 6, 1991, pp. 309-315.

[3] S. Montambault, N. Pouliot, "LineScout Technology: Development of an inspection robot capable of clearing obstacles while operating on a live line," *Proceedings of the 2003 IEEE 10th International Conference in Transmission and Destribution Construction, Operation and Live-line Maintenance*, 2003, pp. 33-40.

[4] G. P. Wu, X. H. Xiao, H. xiao, J. Ch. Dai, Z. L. Huang, "Motion planning of non-collision obstacles overcoming for hing-voltage power transmission-line inspection robot," *Intelligent Robotics and Applications*, springer, Berlin, 2008, pp. 1195-1205.

[5] Z. Z. Liang, E. Li, M. Tan, "Design and control for a tribrachiation motbile robot for the inspection of power transmission lines," *Proceedings of the SICE Annual International Conference on Instrumentation, Control and Information Technology*, Okayama, Japan, 2005, pp. 504-509.

[6] S. Y. Fu, et al., "Structure-constrained obstacles recognition for power transmission line inspection robot," *Proceedings of the IEEE/RSJ International Conference on Intelligent Robots and Systems*, Beijing, China, 2006, pp. 3363-3368.

[7] E. Li, Z. Z. Liang, Z. G. Hou, M. Tan, "Energy-based balance control approach of the ball and beam system. *International Journal of Control*, vol. 82, no. 66, 2009, pp.981-992.

[8] S. Labiod, M. S. Boucherit, T. M. Guerra, "Adaptive fuzzy control of a class of MIMO nonlinear systems," *Fuzzy Sets and Systems*, vol. 151, 2005, pp. 59-77.

[9] L. X. Wang, "Adaptive fuzzy systems and control: design and stability analysis," Printice-Hall, Englewood Cliffs, NJ, 1994.

[10] K. S. Yoo, W. C. Ham, "Adaptive control of robot manipulator using fuzzy compensator," *IEEE Transactions on Fuzzy Systems*, vol. 8, no. 2, 2000, pp. 186-199.